Published in final edited form as:

ACS Chem Biol. 2018 September 21; 13(9): 2663–2672. doi:10.1021/acschembio.8b00578.

Citrullination Inactivates Nicotinamide-*N*-methyltransferase

Venkatesh V. Nemmara[1,2], **Ronak Tilvawala**[1,2], **Ari J. Salinger**[1,2], **Lacey Miller**[1], **Son Hong Nguyen**[1,2], **Eranthie Weerapana**[3], and **Paul R. Thompson**[1,2,*]

[1]Department of Biochemistry and Molecular Pharmacology, UMass Medical School, 364 Plantation Street, Worcester, MA 01605, USA

[2]Program in Chemical Biology, UMass Medical School, 364 Plantation Street, Worcester, MA, 01605, USA.

[3]Department of Chemistry, Boston College, Chestnut Hill, MA 02467

Abstract

Nicotinamide-*N*-methyl transferase (NNMT) catalyzes the irreversible methylation of nicotinamide (NAM) to form *N*-methyl nicotinamide (MeNAM) using SAM as a methyl donor. NNMT is implicated in several chronic disease conditions, including cancers, kidney disease, cardiovascular disease, and Parkinson's disease. Although phosphorylation of NNMT in gastric tumors is reported, the functional effects of this post-translational modification has not been investigated. We previously reported that citrullination of NNMT by Protein Arginine Deiminases (PADs) abolished its methyltransferase activity. Herein, we investigate the mechanism of inactivation. Using tandem MS, we identified three sites of citrullination in NNMT. With this information in hand, we used a combination of site-directed mutagenesis, kinetics, and CD experiments to demonstrate that citrullination of R132 leads to a structural perturbation that ultimately promotes NNMT inactivation.

Abstract

*Author to whom correspondence should be addressed: Department of Biochemistry and Molecular Pharmacology, University of Massachusetts Medical School, LRB 826, 364 Plantation Street, Worcester MA 01605 tel: 508-856-8492; fax: 508-856-6215; paul.thompson@umassmed.edu.

ASSOCIATED CONTENT

Supporting information. Table S1, S2, and S3, and Figures S1-S9. This information is available free of charge via the Internet at http://pubs.acs.org.

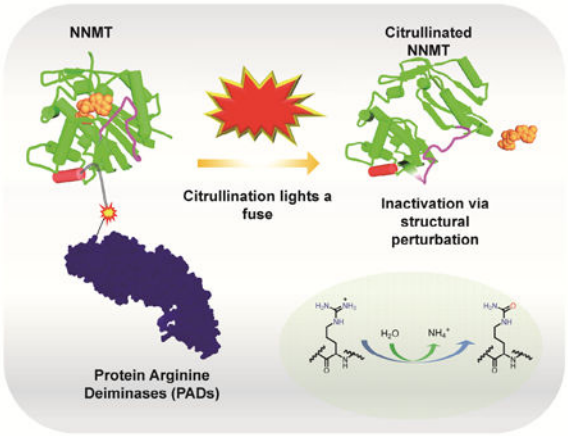

INTRODUCTION

Nicotinamide-*N*-methyl transferase (NNMT) is a cytosolic enzyme that uses *S*-adenosyl methionine (SAM) as a cofactor to catalyze the *N*-methylation of nictotinamide (NAM) to form *N*-methyl nicotinamide (MeNAM) (Figure 1A).[1, 2] NNMT is predominantly expressed in the liver and is also present in kidney, brain, lung, adipose tissues, and muscle.[1, 3–6] NNMT regulates the intracellular levels of SAM and NAM in the methionine cycle and nicotinamide adenine dinucleotide (NAD^+) synthesis pathways, which are crucial controls of cellular energy expenditure.[4, 7] Notably, NNMT is overexpressed in a variety of cancers and metabolic conditions. For example, aberrant NNMT expression is observed in papillary thyroid,[8, 9] gastric,[10] oral, and renal carcinoma,[11, 12] as well as adenocarcinoma,[13, 14] glioblastoma,[15] bladder,[15] colorectal,[16] and lung cancers.[17] Furthermore, increased NNMT expression has been found in the lumbar spinal fluids of patients with Parkinson's disease suggesting a potential role in neurodegenerative diseases.[18, 19] ASO treatment shows efficacy in metabolic diseases confirming the therapeutic potential of targeting this enzyme.[20]

Increased NNMT activity has been shown to regulate the methylation potential in cancer cells by altering SAM and S-adenosylhomocysteine (SAH) concentrations.[21] Despite recent advances, NNMT regulation in cancers and other metabolic disorders like diabetes, remains poorly understood. Many enzymes undergo post-translational modifications and the activity of a clear majority of them are regulated through these modifications.[22, 23] Post-translational modification of NNMT was first reported by Lim *et al.*[24] The authors showed that NNMT is phosphorylated in gastric tumors and demonstrated that casein kinase 2 efficiently phosphorylates recombinant NNMT. However, the mechanism and impact of such a modification was not explored.

Our recent proteomic datasets revealed that NNMT is citrullinated in synovial tissue samples obtained from patients with rheumatoid arthritis (RA).[25] Citrullination is a post-translational modification wherein a peptidyl-arginine is hydrolyzed to form peptidyl-citrulline (Figure 1B).[26, 27] This deimination reaction is catalyzed by the calcium dependent Protein Arginine Deiminases (PADs).[26, 27] The PAD superfamily includes five mammalian isozymes, PADs

1–4 and 6. Of these enzymes, PADs 1–4 have deiminase activity whereas PAD6 is catalytically inactive due to various mutations.[26] Although highly related, PADs display unique cellular and tissue distribution patterns throughout the body.[26–29] Specifically, PAD1 and PAD3 are principally expressed in skin and hair follicles,[28] PAD2 and PAD4 are expressed in neutrophils and myeloid cells[26, 30] and PAD6 is expressed in oocytes and embryos.[31, 32] PADs citrullinate numerous proteins including filaggrin, keratin, and vimentin.[33] In addition, PAD1 has been shown to promote tumorigenesis by regulating MEK1-ERK1/2-MMP2 signaling in triple negative breast cancer.[34] PAD2 is upregulated in multiple sclerosis and in breast cancers.[35, 36] PAD2 is also released into the synovial joints of patients with RA, leading to the citrullination of multiple protein targets, which promotes the generation of anti-citrullinated protein antibodies (ACPA), a characteristic feature of RA.[37, 38]

Since abnormal PAD activity is associated with a variety of autoimmune diseases, including RA, ulcerative colitis, lupus, and multiple sclerosis as well as various cancers,[30, 31] the PADs are potential therapeutic targets.[39, 40] We recently demonstrated that citrullination of Serine Protease Inhibitors (SERPIN) can abolish their ability to inhibit their cognate proteases.[25] We also established that NNMT citrullination abolished its methyltransferase activity.[25] Here, we report a detailed analysis of NNMT citrullination by PAD1 and PAD2 and its effect on NNMT structure and function. Specifically, we show that citrullination destabilizes the protein, which ultimately leads to NNMT inactivation.

RESULTS AND DISCUSSION

Effect of citrullination on the methyl transferase activity of NNMT.

Our previous study showed that citrullination of NNMT by PAD1 and PAD2 completely abolished its methyltransferase activity when either SAM or quinoline were evaluated as the varied substrates (Figure 1C).[25] By contrast, citrullination of NNMT by either PAD3 or PAD4 only led to a moderate reduction in activity. Note that NNMT activity was measured using the alternative substrate quinoline (Figure S1A)[41] and monitoring the formation of 1-methylquinolinium by fluorescence (Figure S1B).[42]

To gain insights into the mechanism of NNMT inactivation, we first determined the steady-state kinetic parameters for PAD mediated citrullination. To identify optimal assay conditions, we first citrullinated wild type NNMT with increasing concentrations of PAD1 and PAD2. The extent of citrullination was determined by rhodamine phenylglyoxal (Rh-PG) labeling (Figure S2A).[43] Next, we generated progress curves of NNMT citrullination to identify the linear range of PAD activity (Figure 2A and B). Subsequently, we measured the initial rates for the citrullination of NNMT (Figure 2C and D). Note that a standard curve was generated to convert the fluorescence intensity of Rh-PG into citrulline concentration (Figure S3A and B).[43] From these experiments, we obtained k_{cat}/K_m values of 4600 $M^{-1}s^{-1}$ and 3500 $M^{-1}s^{-1}$ for PAD1 and PAD2 respectively. Although these values are comparable to other known substrates, e.g., histone H3 (k_{cat}/K_m = 4800 $M^{-1}s^{-1}$) and BAEE (k_{cat}/K_m = 1500 $M^{-1}s^{-1}$), it should be noted that the k_{cat} and K_m values for PAD1 (k_{cat} = 0.014 ± 0.01 s^{-1}; K_m= 3.0 ± 0.8 μM) and PAD2 (k_{cat} = 0.007 ± 0.002 s^{-1}; K_m= 2.0 ± 0.1 μM) are 50- to 100-fold lower than typically observed;[43, 44] the lower K_m value compensates for the

decreased k_{cat} such that k_{cat}/K_m values are similar. Given that PADs citrullinate NNMT in a time-dependent manner and citrullination abolishes its methyltransferase activity, we next investigated the dose dependent inactivation of NNMT by PAD1 and PAD2 (Figure S2B). From these experiments we obtained IC_{50} values of 0.25 μM for PAD1 and 0.8 μM for PAD2 suggesting that both PAD1 and PAD2 inactivate NNMT in a concentration dependent manner.

Identification of citrullination sites in NNMT.

Having established that citrullination abolishes NNMT activity, we then identified the sites of citrullination in NNMT. Since protein citrullination increases the mass of a peptide fragment by only 0.98 Da, it is difficult to unambiguously identify citrullination sites in a protein.[45] Therefore, we employed a novel chemical labeling approach to identify the citrullination sites in NNMT. For these experiments, we citrullinated NNMT and then labeled the protein with phenylglyoxal (PG). PG selectively modifies citrullinated residues under acidic conditions[46, 47] and the modified peptides show a mass increase of 117 Da (Figure 3A). PG modified sites can therefore be unambiguously interpreted as citrullination sites. We used Neutrophil Elastase (NE) for peptide digestion instead of the commonly used Trypsin. Trypsin cleaves peptides after arginine and lysine residues, but generally not after citrulline residues. By contrast, NE cleaves after alanine and valine residues thereby making it an optimal choice for peptide digestion. NE digested peptides were then subjected to chromatography coupled with tandem mass spectrometry analysis. Sequence coverage of NNMT was 85%, and included all nine arginine residues in the protein.

The proteomic data identified three PG modified peptide fragments. Figure 3B shows the sequence of these peptide fragments with PG-modified citrulline residues at positions R18, R132 and R181. The corresponding arginine residues in the control sample did not show a mass change of +117.0102 Da. Figure 3C depicts a representative high-resolution MS/MS spectrum for the citrullination of R132 that unambiguously confirmed PG modification of this residue.

Determining the role of citrullinated residues in NNMT.

To probe the role of citrullinated residues in abolishing NNMT activity, we generated constructs encoding arginine to lysine residues for all nine arginines in NNMT (Figure 4A). We expressed and purified all mutant enzymes and analyzed their methyltransferase activity. Interestingly, all mutants except R132K showed comparable methyltransferase activity to that of wild type NNMT. As depicted in Figure 4B, R132K exhibits a 5-fold reduction in the k_{cat}/K_m value for both SAM and quinoline. Next, we confirmed that these NNMT mutants are also PAD substrates by treating them with PAD1 or PAD2 followed by labeling with Rh-PG. As depicted in Figure S4, all NNMT mutants showed efficient citrullination by PADs 1 and 2. These data are consistent with our findings that at least three residues in NNMT can be citrullinated.

Given that PADs efficiently citrullinate both wild type NNMT and mutant enzymes, we examined the effect of citrullination on the methyltransferase activity of the NNMT mutants. Mutants were citrullinated with either PAD1 or PAD2 and their methyltransferase activity

was measured and compared with the uncitrullinated controls treated under the same condition (Figures 4C, 4D, S5, and S6 and Tables S1 and S2). All of the uncitrullinated arginine mutants, except R132K, retained ≥ 80% of their methyltransferase activity. Uncitrullinated R132K, like its citrullinated counterpart, lost its methyltransferase activity. R132 is one of the citrullination sites identified in our mass spectrometric dataset along with R18 and R181. It is interesting to note that uncitrullinated R18K and R181K did not lose their methyltransferase activity. This data suggests that R132 is essential for the methyltransferase activity of NNMT.

Next, we determined the rate of inactivation of citrullinated R18K, R132K and R181K and compared them with their uncitrullinated controls (Figures 4E, 4F, and S7). We hypothesized that if R132 is the only residue responsible for the loss of NNMT activity upon citrullination, then the rate of inactivation of uncitrullinated and citrullinated R132K will remain the same. Indeed, the obtained rate constants of inactivation for citrullinated (k = 0.01 s^{-1}) and uncitrullinated (k = 0.012 s^{-1}) R132K mutant are quite similar. In stark contrast, the rates of inactivation of citrullinated R18K and R181K are roughly 10-fold higher than the uncitrullinated controls (Figures 4F, and Table 1). Taken together, these results clearly demonstrate that despite multiple sites of citrullination, modification of R132 leads to NNMT inactivation.

Structural basis of inactivation.

To gain insights into the structural role of R132, we analyzed the crystal structure of NNMT (PDB ID: 3ROD). NNMT is a class-I SAM dependent methyltransferase comprised of a seven-stranded β-sheet flanked by eight α-helices on both sides that are connected by ten loops.[48–50] The ternary complex of NNMT bound to its substrate NAM and *S*-adenosyl homocysteine (SAH)[51] shows that the adenine ring of SAH makes hydrophobic interactions with the sidechains of Y86 from helix-4 and A169 from helix-7 (Figures 5 and S8). Moreover, it also makes hydrogen bonding interactions with the sidechain of D142 and the backbone amide of V143 (Figure S8), which are anchored on loop-7.[51] Molecular dynamics simulations on the NNMT mutant D197A suggested that loop-7, which is formed by residues V138-L154, undergoes a major conformational change relative to wildtype. Such a change results in decreased binding of SAH to the mutant enzyme.[51] As shown in Figure 5A, loop −7 is connected to helix-6 through a β-strand. Notably, R132 from helix-6 interacts with E128 and E129 of the same helix via electrostatic interactions. R132 also makes a cationic-π interaction with the indole ring of W97 from helix-4. (Figure 5B). Additionally, the ε-nitrogen of R132 hydrogen bonds with the backbone carbonyl oxygen of W97. These interactions exhibited by the positively charged R132 with helix-4 are important because any disruption would likely result in a structural perturbation. Such a structural perturbation would destabilize loop-7, which would be expected to impact SAM binding. Furthermore, the loss of an interaction between helix-4 and helix-6 could in turn disrupt interactions of residues Y86 and S87 with SAM (Figure S8). Taken together, these data suggest that citrullination of R132 destabilizes NNMT, which subsequently leads to enzyme inactivation.

Consistent with this hypothesis is the fact that the rate of inactivation of the R132K mutant with and without a PAD are nearly identical. The lysine mutant is intrinsically destabilized

due to the inability of a lysine to fully substitute for the network of interactions afforded by R132. Based on these observations, it is likely that the methyltransferase activity of citrullinated NNMT is abolished due to structural perturbations resulting from the loss of positive charge on R132. To further confirm this hypothesis, we generated alanine (R132A) and glutamine (R132Q) mutants. Interestingly, neither of these mutants were found in soluble fractions. In addition, the insoluble fractions did not possess methyltransferase activity (Figure S9), suggesting that R132 is important residue for folding and for maintaining the secondary structure of the protein.

To further probe the role of R132 in maintaining the secondary structure of NNMT we used circular dichroism (CD) spectroscopy. For these studies we measured the far UV CD-spectra of wild type NNMT under three different conditions: without incubation, and incubated at 37 °C in the presence and absence of PAD1. The spectrum of wild type NNMT by itself has strong minima at 230 nm, which do not change significantly for the uncitrullinated enzyme incubated at 37 °C. However, citrullinated NNMT show a 30% reduction in the molar ellipticity at 230 nm (Figure 5C). This result indicates that the secondary structure of the citrullinated enzyme is perturbed upon citrullination. We also carried out the same experiments with the R132K mutant (Figure 5D). The mutant enzyme without incubation displayed strong minima at 230 nm with 90% of the ellipticity of the wild type enzyme. The uncitrullinated and citrullinated mutant incubated in the absence and presence of PAD1 showed a decrease in molar ellipticity at 230 nm by 40% and 38%, respectively. These results are also consistent with the hypothesis that citrullination destabilizes the protein leading to its inactivation.

Conclusions.

In summary, we report that NNMT activity is regulated by citrullination. Using tandem mass spectrometry along with site-directed mutagenesis and kinetics, we explored the detailed mechanism of inactivation of citrullinated NNMT. Mass spectrometry experiments identified three citrullination sites in NNMT, of which, R132 was found to be essential for maintaining NNMT activity. Furthermore, CD experiments revealed that citrullination results in a structural perturbation of NNMT. Although we cannot definitively rule out an effect on cofactor binding, citrullination of the R132K mutant does not enhance its rate of inactivation, which indicates that the loss of activity is due to the loss of an optimized interaction. Moreover, the R132K mutation does not affect the K_m for SAM. Therefore, we conclude that R132 citrullination results in the loss of crucial interactions that maintain the structural integrity of NNMT. Taken together, these data indicate that R132 citrullination lights a fuse that ultimately leads to NNMT inactivation via a loss in structural integrity. NNMT is overexpressed in numerous cancers and high levels are known to alter the SAM/SAH ratio in cells, which can have profound effects on DNA and histone methylation. Notably, a recent study showed that NNMT overexpression promotes a pro-growth phenotype.[21] Since citrullination abolishes NNMT activity, the PADs may downregulate NNMT activity in a subset of tumors. Consistent with that possibility is the fact that PAD2 act as a tumor suppressor in a subset of breast cancers.[52] Overall, these results provide insights into the regulation of NNMT activity via citrullination under physiological conditions.

METHODS

Materials.

PADs 1, 2, 3 and 4 were purified as reported.[44, 53] Rhodamine-phenylglyoxal (Rh-PG) was synthesized as reported.[43] The plasmid pET28a-LIC, harboring the *NNMT* gene was purchased from Addgene (Addgene plasmid # 40734). All chemicals were purchased from Sigma.

Site-directed mutagenesis.

The pET28:NNMT vector was used as a template for generating all arginine to lysine mutations. Primers used for mutating the individual arginine residues are shown in Table S3. PCR reactions were performed under standard conditions using the respective primers along with *iProof* high-fidelity DNA polymerase (*BIO-RAD*) in GC buffer and dNTPs in the reaction mixture. The PCR product was analyzed on a 1% (w/v) agarose gel and the amplification product was incubated with 10 units of Dpn1 for 2 h at 37 °C. The product was then transformed into *E. coli* BL21(DE3) host cells and single colonies were selected. DNA sequencing of the insert gene confirmed the desired mutation. Expression and purification of the mutants were performed as described for the wild-type enzyme (see below).

Purification of recombinant human NNMT.

Human NNMT was purified using the methodology outlined below. Briefly, a pET28 vector encoding human NNMT was transformed into BL21(DE3) cells and grown in 2 L of Terrific Broth (TB) containing 50 μg/mL of kanamycin to an OD of 0.6–0.8 at 37 °C diluted 1:10 from an overnight culture. Protein expression was induced with 1.0 mM IPTG for 16–18 h at 16 °C. The cells were pelleted by centrifugation, resuspended in lysis buffer (50 mM Tris pH 8.0, 300 mM NaCl, 5 mM imidazole, 2 mM β-mercaptoethanol, 1 mM PMSF) before sonication. The lysate was centrifuged and the supernatant containing soluble NNMT was incubated with Ni-NTA resin (GE biosciences). The resin was washed twice with lysis buffer containing 30 mM and 70 mM of imidazole, respectively, and the protein was eluted with 250 mM of imidazole. The protein was further dialyzed overnight at 4 °C in dialysis buffer (50 mM Tris pH 8.0, 300 mM NaCl, 5% glycerol, and 1 mM DTT) to remove imidazole. The dialyzed fractions were concentrated to obtain 4 mg/mL protein aliquots and were flash frozen using liquid nitrogen. The Bradford assay was used to determine protein concentrations.

Human NNMT activity assay.

Human NNMT activity assays were carried out in two different scenarios using quinoline as the substrate and SAM as the coenzyme. To measure NNMT activity against quinoline, citrullinated and uncitrullinated NNMT were added to individual wells of a 96-well plate (final concentration 0.6 μM (60 μL) containing various quinoline concentrations (0, 10, 20, 40, 60, and 80, and 100 μM) and a fixed SAM concentration (100 μM). The assay contained buffer composed of 5 mM Tris pH 8.6 and 1 mM DTT. To measure NNMT activity against SAM, citrullinated and uncitrullinated NNMT were added to individual wells of a 96-well plate (final concentration 0.6 μM, 60 μL) containing various SAM concentrations (0, 10, 20,

40, 60, and 100, and 140 μM) and a fixed quinoline concentration (100 μM) in assay. The initial velocity proportional to enzymatic activity was measured by monitoring the formation of 1-methylquinolinium fluorometrically (λ ex = 330 nm; λ em = 405 nm). The initial rates obtained from these assays were fit by nonlinear least fit squares to equation 1,

$$v = V_{max}[S]/K_M + [S] \quad \text{Eq 1},$$

using the GraphPad Prism 7.0 software package and kinetic parameters were calculated. The experiment was carried out in duplicate.

Detection of citrullination sites in NNMT.

Pure NNMT was labelled with phenylglyoxal similarly to previously described methods.[43] Briefly, NNMT (100 μg) was first citrullinated by incubating at 37 °C in 100 mM HEPES pH 7.6, 100 mM NaCl, 500 μM TCEP, and 1 mM $CaCl_2$ with PAD1 or PAD2 (100 μg) for 2 h. As a control, NNMT was incubated under the same conditions in the absence of a PAD. Citrullinated proteins were then incubated with 20% trichloroacetic acid (TCA) (40 μL of 100% TCA) and phenylglyoxal (250 μM) for 3 h at 37 °C. Next, the labeling reaction was quenched with 25 μL of 0.5 M citrulline dissolved in 50 mM HEPES pH 7.6. The solutions were then placed on ice for 30 min followed by centrifugation (13,500 rpm, 15 min) at 4 °C. The supernatants were discarded, and the protein pellets were washed twice with cold acetone and dried. The protein pellets were then sonicated and resolubilized in 6 M urea (30 μL) and 100 mM ammonium bicarbonate (70 μL) solution. Once dissolved, the samples were incubated with 1 M DTT (1.5 μL) for 15 min at 65 °C followed by incubation with 500 mM iodoacetamide (2.5 μL) for 30 min at RT. After 30 min, the samples were diluted to 1 mL final volume with PBS to bring down the urea concentration to ~2 M. The samples were then treated with neutrophil elastase (3 μL, 1:20 dilution) overnight at 37 °C. The samples were dried using a speedVac and further subjected to three spin column washes. The eluted samples were further dried using a speedVac, resolubilized in Buffer A (95% ACN, 5 % water and 0.5 % formic acid) and stored at −20 °C until MS analysis.

LC/LC-MS/MS and data processing.

LC-MS/MS analysis was performed on an LTQ-Orbitrap Discovery mass spectrometer (ThermoFisher) coupled to an Agilent 1200 series HPLC. Samples were loaded via HPLC autosampler onto a hand-pulled 100 μm fused-silica capillary column with a 5 μm tip packed with 10 cm Aqua C18 reverse phase resin (Phenomenex). Peptides were eluted over a 5 h elution using a gradient from 100% Buffer A (95% water, 5% acetonitrile, 0.1% formic acid) to 100% Buffer B (20% water, 80% acetonitrile, 0.1% formic acid). The flow rate through the column was set to ~0.25 μL/min and the spray voltage was set to 2.75 kV. One full MS scan was followed by 8 data dependent scans of the 8 most abundant ions. For high resolution runs, a full scan was followed by 4 data dependent scans limited to an inclusion mass list containing the masses of previously identified modified peptides. The tandem MS data were searched using the SEQUEST algorithm using a concatenated target/decoy variant of the human UniProt database. A static modification of +57.02146 on cysteine was specified to account for alkylation by iodoacetamide and a differential modification of

+117.0102 was specified on arginine. SEQUEST output files were filtered using DTA-Select.

Detection of NNMT citrullination by rhodamine-PG labeling.

Protein citrullination was carried out as described previously.[46] Briefly, NNMT (6 μM) was incubated in buffer (100 mM HEPES pH 7.6, 100 mM NaCl, 500 μM TCEP, 1 mM $CaCl_2$) with or without PAD (0, 0.125, 0.5, 1, 2, and 4 μM) at 37 °C for 2 h. The samples were then incubated with 20% TCA (10 μL of 100% TCA) and 0.1 mM rhodamine-PG (1 μL of 5 mM stock) for 30 min at 37 °C. After a 30 min incubation, the reaction was quenched with citrulline (0.1 M final concentration) dissolved in 50 mM HEPES pH 7.6. The solutions were placed on ice for 30 min followed by centrifugation (13,500 rpm, 15 min) at 4 °C. The supernatants were discarded, and the protein pellets were washed twice with cold acetone and dried. To eliminate arginine labeling, the pellet was dissolved in 20 μL of buffer containing 20 mM HEPES pH 8.0, 100 mM arginine, 1% SDS, 7% β-mercapto ethanol, and 100 mM NaCl. The samples were further boiled with 6X SDS loading dye and sonicated for 15 min and separated by SDS-PAGE (12.5% gel). Bands were visualized by scanning the gel in a typhoon scanner (approximate excitation/emission maxima ~546/579, respectively).

Time dependent NNMT citrullination visualized by Rh-PG.

Time dependent citrullination of NNMT was carried out by incubating NNMT (6 μM) in buffer (100 mM HEPES pH 7.6, 100 mM NaCl, 500 μM TCEP, 1 mM $CaCl_2$) with or without a PAD (final concentration 0.7 μM) at 37 °C for various time intervals (0, 15, 30, 45, 60, 75, 90, 105, and 120 min) and flash frozen to stop the reaction. The samples were then incubated with 20% TCA (10 μL of 100% TCA) and 0.1 mM rhodamine-PG (1 μL of 5 mM stock) for 30 min at 37 °C. After a 30 min incubation, the reaction was quenched with 10 μL of 0.5 M citrulline dissolved in 50 mM HEPES pH 7.6. The solutions were placed on ice for 30 min followed by centrifugation (13,500 rpm, 15 min) at 4 °C. The supernatants were discarded, and the protein pellets were washed twice with cold acetone and dried. To eliminate arginine labeling, the pellet was dissolved in 20 μL of buffer containing 20 mM HEPES pH 8.0, 100 mM arginine, 1% SDS, 7% β-mercapto ethanol, and 100 mM NaCl. The samples were further boiled with 6X SDS loading dye and sonicated for 15 min and separated by SDS-PAGE (12.5% gel). Bands were visualized by scanning the gel in a typhoon scanner (approximate excitation/emission maxima ~546/579, respectively). The experiment was carried out in duplicate, the band intensities were quantified and the data were fit to equation 2, using GraphPad Prism 7.0 software package.

$$F = F_0\left(1 - e^{-kt}\right) \quad \text{Eq 2}$$

F is the normalized fluorescence intensity and F_0 is the normalized fluorescence intensity at time zero. k is the pseudo-first order rate constant of NNMT citrullination by PADs and t is time.

NNMT inactivation as a function of PAD concentration.

NNMT (6 μM) was incubated in buffer (100 mM HEPES pH 7.6, 100 mM NaCl, 500 μM TCEP, 1 mM $CaCl_2$) with or without a PAD (0, 0.125, 0.5, 1, 2, and 4 μM) at 37 °C for 2 h. Methyltransferase activity was evaluated with PAD-treated NNMT as described above. The experiment was carried out in duplicate. The IC_{50} values were then determined by fitting the activity data to equation 3,

$$\text{Percent activity} = 100/\left(1 + [\text{I}]/\text{IC}_{50}\right) \quad \text{Eq 3}$$

using the GraphPad Prism 7.0 software package, where [I] is the concentration of a PAD.

Time dependent inactivation of citrullinated NNMT

Time dependent NNMT citrullination was carried out as described above. Aliquots were removed at various time intervals (0, 15, 30, 45, 60, 75, 90, 105, and 120 min) and assayed for methyltransferase activity as described above. The experiment was carried out in duplicate, the data plotted as a function of time and were fit to equation 4,

$$A = A_0\, e^{-kt} \quad \text{Eq 4}$$

using the GraphPad Prism 7.0 software package. A is the percent activity and A_0 is the percent activity at time zero. k is the pseudo-first order rate constant of inactivation of citrullinated NNMT and t is time.

Steady-state kinetics of PAD1 and PAD2 with NNMT as a substrate.

For kinetic measurements, a standard curve was generated with different concentrations of citrullinated histone H3. Briefly, histone H3 (100 μM) was treated with PAD4 (0.2 μM) in reaction buffer at 37 °C for 1 h. Samples were then treated with 20% TCA and 0.1 mM Rh-PG at 37 °C for 30 min. All samples were quenched with citrulline, cooled, centrifuged, washed and dried, as described above. After resuspending in 50 mM HEPES, samples were separated by SDS-PAGE (15%; 170 V; 50 min) and imaged on a Typhoon scanner (approximate excitation/emission maxima ~546/579, respectively). Images were analyzed using ImageJ and the band intensities fit to equation 5,

$$y = mx + c \quad \text{Eq 5}$$

where m is the slope of the line and c is the intercept.

For the kinetic assay, varying concentrations of both NNMT (0, 0.375, 0.75, 1.5, 3, 6, and 12 μM) were treated with PAD1 (0.2 μM) or PAD2 (0.4 μM) in reaction buffer at 37 °C for 20 min. Reactions were then treated with 20% TCA and 0.1 mM Rh-PG at 37 °C for 30 min. All samples were quenched with citrulline, cooled, centrifuged, washed and dried as described above. After resuspending in 20 mM HEPES pH 8.0, 100 mM arginine, 1% SDS,

7% β-mercapto ethanol, and 100 mM NaCl. Samples were separated by SDS-PAGE and imaged on a Typhoon scanner (approximate excitation/emission maxima ~546/579, respectively). Images were analyzed using ImageJ and the initial rates fit to equation 1 using the GraphPad Prism 7.0 software package. The experiment was carried out in duplicate.

CD measurements

CD measurements were carried out on a Jasco Model J-810 spectropolarimeter equipped with a thermoelectric temperature control system in a 1 cm cuvette (Hellma). Using a 1 cm path length and a 2.5 nm bandwidth, the data were in wavelength scanning mode, recording every 1 nm from 215 to 265 nm, with an 8 s averaging time. For sample preparation, NNMT or the R132K mutant (5 μM), treated with or without PAD1 (0.1 μM), were incubated at 37 °C for 2 h (50 mM HEPES pH 7.6, 500 μM TCEP, and 1 mM $CaCl_2$). As a control, NNMT or the R132K mutant (5 μM) were used directly without any incubation at 37 °C for 2 h. All samples were filtered through a 0.2 μM filter to remove any aggregates and the samples were diluted to 2 μM for recording CD spectra. The Bradford assay was used to determine protein concentrations. Data obtained for PAD1 alone was subtracted from the PAD1 treated samples. Final data was converted to molar ellipticity using equation 6,

$$[\theta]\lambda = (\mathrm{MRW}\cdot\theta\lambda)/(10 \cdot d \cdot c) \quad \text{Eq 6}$$

where MRW is the mean residue ellipticity, c is the concentration in g/mL and d is the pathlength in cm.

Supplementary Material

Refer to Web version on PubMed Central for supplementary material.

ACKNOWLEDGEMENTS

This work was supported in part by NIH grant R35GM118112 (P.R.T.). We would like to thank R.C. Mathews and R. Jain for their help with the CD experiments.

ABBREVIATIONS

RA	Rheumatoid arthritis
PAD	Protein arginine deiminase
ACPA	Anti-citrullinated protein antibodies
TCA	trichloroacetic acid
NNMT	Nicotinamide-N-methyl transferase
NAM	nicotinamide
MeNAM	N-methyl nicotinamide
ASO	Antisense oligonuncelotides

References.

(1). Rini J, Szumlanski C, Guerciolini R, and Weinshilboum RM (1990) Human liver nicotinamide N-methyltransferase: ion-pairing radiochemical assay, biochemical properties and individual variation, Clin Chim Acta 186, 359–374. [PubMed: 2311261]

(2).) Aksoy S, Szumlanski CL, and Weinshilboum RM (1994) Human liver nicotinamide N-methyltransferase. cDNA cloning, expression, and biochemical characterization, J Biol Chem 269, 14835–14840. [PubMed: 8182091]

(3).) Cantoni GL (1951) Methylation of nicotinamide with soluble enzyme system from rat liver, J Biol Chem 189, 203–216. [PubMed: 14832232]

(4).) Kraus D, Yang Q, Kong D, Banks AS, Zhang L, Rodgers JT, Pirinen E, Pulinilkunnil TC, Gong F, Wang YC, Cen Y, Sauve AA, Asara JM, Peroni OD, Monia BP, Bhanot S, Alhonen L, Puigserver P, and Kahn BB (2014) Nicotinamide N-methyltransferase knockdown protects against diet-induced obesity, Nature 508, 258–262. [PubMed: 24717514]

(5).) Alston TA, and Abeles RH (1988) Substrate specificity of nicotinamide methyltransferase isolated from porcine liver, Arch Biochem Biophys 260, 601–608. [PubMed: 2963591]

(6).) Yan L, Otterness DM, Craddock TL, and Weinshilboum RM (1997) Mouse liver nicotinamide N-methyltransferase: cDNA cloning, expression, and nucleotide sequence polymorphisms, Biochem Pharmacol 54, 1139–1149. [PubMed: 9464457]

(7).) Riederer M, Erwa W, Zimmermann R, Frank S, and Zechner R (2009) Adipose tissue as a source of nicotinamide N-methyltransferase and homocysteine, Atherosclerosis 204, 412–417. [PubMed: 18996527]

(8).) Xu J, Moatamed F, Caldwell JS, Walker JR, Kraiem Z, Taki K, Brent GA, and Hershman JM (2003) Enhanced expression of nicotinamide N-methyltransferase in human papillary thyroid carcinoma cells, J Clin Endocrinol Metab 88, 4990–4996. [PubMed: 14557485]

(9).) Xu J, Capezzone M, Xu X, and Hershman JM (2005) Activation of nicotinamide N-methyltransferase gene promoter by hepatocyte nuclear factor-1beta in human papillary thyroid cancer cells, Mol Endocrinol 19, 527–539. [PubMed: 15486044]

(10).) Chen C, Wang X, Huang X, Yong H, Shen J, Tang Q, Zhu J, Ni J, and Feng Z (2016) Nicotinamide N-methyltransferase: a potential biomarker for worse prognosis in gastric carcinoma, Am J Cancer Res 6, 649–663. [PubMed: 27152242]

(11).) Sartini D, Muzzonigro G, Milanese G, Pierella F, Rossi V, and Emanuelli M (2006) Identification of nicotinamide N-methyltransferase as a novel tumor marker for renal clear cell carcinoma, J Urol 176, 2248–2254. [PubMed: 17070307]

(12).) Tang SW, Yang TC, Lin WC, Chang WH, Wang CC, Lai MK, and Lin JY (2011) Nicotinamide N-methyltransferase induces cellular invasion through activating matrix metalloproteinase-2 expression in clear cell renal cell carcinoma cells, Carcinogenesis 32, 138–145. [PubMed: 21045016]

(13).) Mobley A, Zhang S, Bondaruk J, Wang Y, Majewski T, Caraway NP, Huang L, Shoshan E, Velazquez-Torres G, Nitti G, Lee S, Lee JG, Fuentes-Mattei E, Willis D, Zhang L, Guo CC, Yao H, Baggerly K, Lotan Y, Lerner SP, Dinney C, McConkey D, Bar-Eli M, and Czerniak B (2017) Aurora Kinase A is a Biomarker for Bladder Cancer Detection and Contributes to its Aggressive Behavior, Sci Rep 7, 40714. [PubMed: 28102366]

(14).) Fahrmann JF, Grapov DD, Wanichthanarak K, DeFelice BC, Salemi MR, Rom WN, Gandara DR, Phinney BS, Fiehn O, Pass H, and Miyamoto S (2017) Integrated Metabolomics and Proteomics Highlight Altered Nicotinamide- and Polyamine Pathways in Lung Adenocarcinoma, Carcinogenesis *DOI:* 10.1093/carcin/bgw205.

(15).) Palanichamy K, Kanji S, Gordon N, Thirumoorthy K, Jacob JR, Litzenberg KT, Patel D, and Chakravarti A (2017) NNMT Silencing Activates Tumor Suppressor PP2A, Inactivates Oncogenic STKs, and Inhibits Tumor Forming Ability, Clin Cancer Res 23, 2325–2334. [PubMed: 27810903]

(16).) Roessler M, Rollinger W, Palme S, Hagmann ML, Berndt P, Engel AM, Schneidinger B, Pfeffer M, Andres H, Karl J, Bodenmuller H, Ruschoff J, Henkel T, Rohr G, Rossol S, Rosch W, Langen

H, Zolg W, and Tacke M (2005) Identification of nicotinamide N-methyltransferase as a novel serum tumor marker for colorectal cancer, Clin Cancer Res 11, 6550–6557. [PubMed: 16166432]

(17).) Tomida M, Mikami I, Takeuchi S, Nishimura H, and Akiyama H (2009) Serum levels of nicotinamide N-methyltransferase in patients with lung cancer, J Cancer Res Clin Oncol 135, 1223–1229. [PubMed: 19242722]

(18).) Parsons RB, Smith SW, Waring RH, Williams AC, and Ramsden DB (2003) High expression of nicotinamide N-methyltransferase in patients with idiopathic Parkinson's disease, Neurosci Lett 342, 13–16. [PubMed: 12727306]

(19).) Aoyama K, Matsubara K, Kondo M, Murakawa Y, Suno M, Yamashita K, Yamaguchi S, and Kobayashi S (2001) Nicotinamide-N-methyltransferase is higher in the lumbar cerebrospinal fluid of patients with Parkinson's disease, Neurosci Lett 298, 78–80. [PubMed: 11154840]

(20).) Cao Y, Matsubara T, Zhao C, Gao W, Peng L, Shan J, Liu Z, Yuan F, Tang L, Li P, Guan Z, Fang Z, Lu X, Huang H, and Yang Q (2017) Antisense oligonucleotide and thyroid hormone conjugates for obesity treatment, Sci Rep 7, 9307. [PubMed: 28839185]

(21).) Ulanovskaya OA, Zuhl AM, and Cravatt BF (2013) NNMT promotes epigenetic remodeling in cancer by creating a metabolic methylation sink, Nat Chem Biol 9, 300–306. [PubMed: 23455543]

(22).) Perkins ND (2006) Post-translational modifications regulating the activity and function of the nuclear factor kappa B pathway, Oncogene 25, 6717–6730. [PubMed: 17072324]

(23).) Walsh G, and Jefferis R (2006) Post-translational modifications in the context of therapeutic proteins, Nat Biotechnol 24, 1241–1252. [PubMed: 17033665]

(24).) Lim BH, Cho BI, Kim YN, Kim JW, Park ST, and Lee CW (2006) Overexpression of nicotinamide N-methyltransferase in gastric cancer tissues and its potential post-translational modification, Exp Mol Med 38, 455–465. [PubMed: 17079861]

(25).) Tilvawala R, Nguyen SH, Maurais AJ, Nemmara VV, Nagar M, Salinger AJ, Nagpal S, Weerapana E, and Thompson PR (2018) The Rheumatoid Arthritis-Associated Citrullinome, Cell Chem Biol 25, 691–704. [PubMed: 29628436]

(26).) Fuhrmann J, Clancy KW, and Thompson PR (2015) Chemical biology of protein arginine modifications in epigenetic regulation, Chem Rev 115, 5413–5461. [PubMed: 25970731]

(27).) Nemmara VV, Subramanian V, Muth A, Mondal S, Salinger AJ, Maurais AJ, Tilvawala R, Weerapana E, and Thompson PR (2018) The Development of Benzimidazole-Based Clickable Probes for the Efficient Labeling of Cellular Protein Arginine Deiminases (PADs), ACS Chem Biol 13, 712–722. [PubMed: 29341591]

(28).) Zhang X, Liu X, Zhang M, Li T, Muth A, Thompson PR, Coonrod SA, and Zhang X (2016) Peptidylarginine deiminase 1-catalyzed histone citrullination is essential for early embryo development, Sci Rep 6, 38727. [PubMed: 27929094]

(29).) Zhang X, Bolt M, Guertin MJ, Chen W, Zhang S, Cherrington BD, Slade DJ, Dreyton CJ, Subramanian V, Bicker KL, Thompson PR, Mancini MA, Lis JT, and Coonrod SA (2012) Peptidylarginine deiminase 2-catalyzed histone H3 arginine 26 citrullination facilitates estrogen receptor alpha target gene activation, Proc Natl Acad Sci U S A 109, 13331–13336. [PubMed: 22853951]

(30).) Bicker KL, and Thompson PR (2013) The protein arginine deiminases: Structure, function, inhibition, and disease, Biopolymers 99, 155–163. [PubMed: 23175390]

(31).) Jones JE, Causey CP, Knuckley B, Slack-Noyes JL, and Thompson PR (2009) Protein arginine deiminase 4 (PAD4): Current understanding and future therapeutic potential, Curr Opin Drug Discov Devel 12, 616–627.

(32).) Esposito G, Vitale AM, Leijten FP, Strik AM, Koonen-Reemst AM, Yurttas P, Robben TJ, Coonrod S, and Gossen JA (2007) Peptidylarginine deiminase (PAD) 6 is essential for oocyte cytoskeletal sheet formation and female fertility, Mol Cell Endocrinol 273, 25–31. [PubMed: 17587491]

(33).) Senshu T, Kan S, Ogawa H, Manabe M, and Asaga H (1996) Preferential deimination of keratin K1 and filaggrin during the terminal differentiation of human epidermis, Biochem Biophys Res Commun 225, 712–719. [PubMed: 8780679]

(34).) Qin H, Liu X, Li F, Miao L, Li T, Xu B, An X, Muth A, Thompson PR, Coonrod SA, and Zhang X (2017) PAD1 promotes epithelial-mesenchymal transition and metastasis in triple-negative breast cancer cells by regulating MEK1-ERK1/2-MMP2 signaling, Cancer Lett 409, 30–41. [PubMed: 28844713]

(35).) Mohanan S, Cherrington BD, Horibata S, McElwee JL, Thompson PR, and Coonrod SA (2012) Potential role of peptidylarginine deiminase enzymes and protein citrullination in cancer pathogenesis, Biochem Res Int 2012, 895343. [PubMed: 23019525]

(36).) McElwee JL, Mohanan S, Griffith OL, Breuer HC, Anguish LJ, Cherrington BD, Palmer AM, Howe LR, Subramanian V, Causey CP, Thompson PR, Gray JW, and Coonrod SA (2012) Identification of PADI2 as a potential breast cancer biomarker and therapeutic target, BMC Cancer 12, 500. [PubMed: 23110523]

(37).) Damgaard D, Senolt L, Nielsen MF, Pruijn GJ, and Nielsen CH (2014) Demonstration of extracellular peptidylarginine deiminase (PAD) activity in synovial fluid of patients with rheumatoid arthritis using a novel assay for citrullination of fibrinogen, Arthritis Res Ther 16, 498. [PubMed: 25475141]

(38).) Burska AN, Hunt L, Boissinot M, Strollo R, Ryan BJ, Vital E, Nissim A, Winyard PG, Emery P, and Ponchel F (2014) Autoantibodies to posttranslational modifications in rheumatoid arthritis, Mediators Inflamm 2014, 492873. [PubMed: 24782594]

(39).) Muth A, Subramanian V, Beaumont E, Nagar M, Kerry P, McEwan P, Srinath H, Clancy K, Parelkar S, and Thompson PR (2017) Development of a Selective Inhibitor of Protein Arginine Deiminase 2, J Med Chem 60, 3198–3211. [PubMed: 28328217]

(40).) Mondal S, Parelkar SS, Nagar M, and Thompson PR (2018) Photochemical Control of Protein Arginine Deiminase (PAD) Activity, ACS Chem Biol 13, 1057–1065. [PubMed: 29517899]

(41).) van Haren MJ, Sastre Torano J, Sartini D, Emanuelli M, Parsons RB, and Martin NI (2016) A Rapid and Efficient Assay for the Characterization of Substrates and Inhibitors of Nicotinamide N-Methyltransferase, Biochemistry 55, 5307–5315. [PubMed: 27570878]

(42).) Neelakantan H, Vance V, Wang HL, McHardy SF, and Watowich SJ (2017) Noncoupled Fluorescent Assay for Direct Real-Time Monitoring of Nicotinamide N-Methyltransferase Activity, Biochemistry 56, 824–832. [PubMed: 28121423]

(43).) Bicker KL, Subramanian V, Chumanevich AA, Hofseth LJ, and Thompson PR (2012) Seeing citrulline: development of a phenylglyoxal-based probe to visualize protein citrullination, J Am Chem Soc 134, 17015–17018. [PubMed: 23030787]

(44).) Knuckley B, Causey CP, Jones JE, Bhatia M, Dreyton CJ, Osborne TC, Takahara H, and Thompson PR (2010) Substrate specificity and kinetic studies of PADs 1, 3, and 4 identify potent and selective inhibitors of protein arginine deiminase 3, Biochemistry 49, 4852–4863. [PubMed: 20469888]

(45).) Clancy KW, Weerapana E, and Thompson PR (2016) Detection and identification of protein citrullination in complex biological systems, Curr Opin Chem Biol 30, 1–6. [PubMed: 26517730]

(46).) Lewallen DM, Bicker KL, Subramanian V, Clancy KW, Slade DJ, Martell J, Dreyton CJ, Sokolove J, Weerapana E, and Thompson PR (2015) Chemical Proteomic Platform To Identify Citrullinated Proteins, ACS Chem Biol 10, 2520–2528. [PubMed: 26360112]

(47).) Choi M, Song JS, Kim HJ, Cha S, and Lee EY (2013) Matrix-assisted laser desorption ionization-time of flight mass spectrometry identification of peptide citrullination site using Br signature, Anal Biochem 437, 62–67. [PubMed: 23499971]

(48).) Kozbial PZ, and Mushegian AR (2005) Natural history of S-adenosylmethionine-binding proteins, BMC Struct Biol 5, 19. [PubMed: 16225687]

(49).) Martin JL, and McMillan FM (2002) SAM (dependent) I AM: the S-adenosylmethionine-dependent methyltransferase fold, Curr Opin Struct Biol 12, 783–793. [PubMed: 12504684]

(50).) Schubert HL, Blumenthal RM, and Cheng X (2003) Many paths to methyltransfer: a chronicle of convergence, Trends Biochem Sci 28, 329–335. [PubMed: 12826405]

(51).) Peng Y, Sartini D, Pozzi V, Wilk D, Emanuelli M, and Yee VC (2011) Structural basis of substrate recognition in human nicotinamide N-methyltransferase, Biochemistry 50, 7800–7808. [PubMed: 21823666]

(52).) Horibata S, Rogers KE, Sadegh D, Anguish LJ, McElwee JL, Shah P, Thompson PR, and Coonrod SA (2017) Role of peptidylarginine deiminase 2 (PAD2) in mammary carcinoma cell migration, BMC Cancer 17, 378. [PubMed: 28549415]

(53).) Causey CP, Jones JE, Slack JL, Kamei D, Jones LE, Subramanian V, Knuckley B, Ebrahimi P, Chumanevich AA, Luo Y, Hashimoto H, Sato M, Hofseth LJ, and Thompson PR (2011) The Development of N-alpha-(2-Carboxyl)benzoyl-N(5)-(2-fluoro-1-iminoethyl)-l-ornithine Amide (o-F-amidine) and N-alpha-(2-Carboxyl)benzoyl-N(5)-(2-chloro-1-iminoethyl)-l-ornithine Amide (o-Cl-amidine) As Second Generation Protein Arginine Deiminase (PAD) Inhibitors, J Med Chem 54, 6919–6935. [PubMed: 21882827]

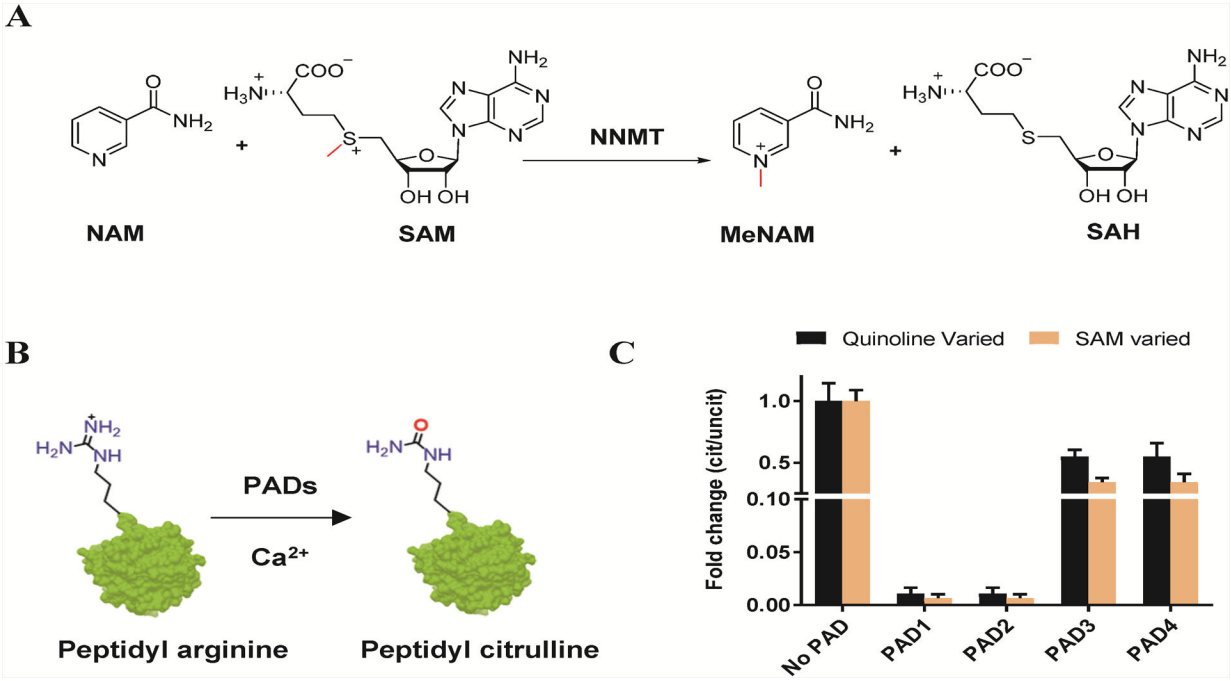

Figure 1.

(**A**) NNMT catalyzed methylation of nicotinamide (NAM) to *N*-methylnicotinamide (MeNAM) in the presence of *S*-adenosylmethionine (SAM). (**B**) PAD-catalyzed hydrolysis of peptidyl-arginine to peptidyl-citrulline. (**C**) Fold change in the k_{cat}/K_M of wild type NNMT (citrullinated/uncitrullinated) after treatment with PAD1, 2, 3, or 4.

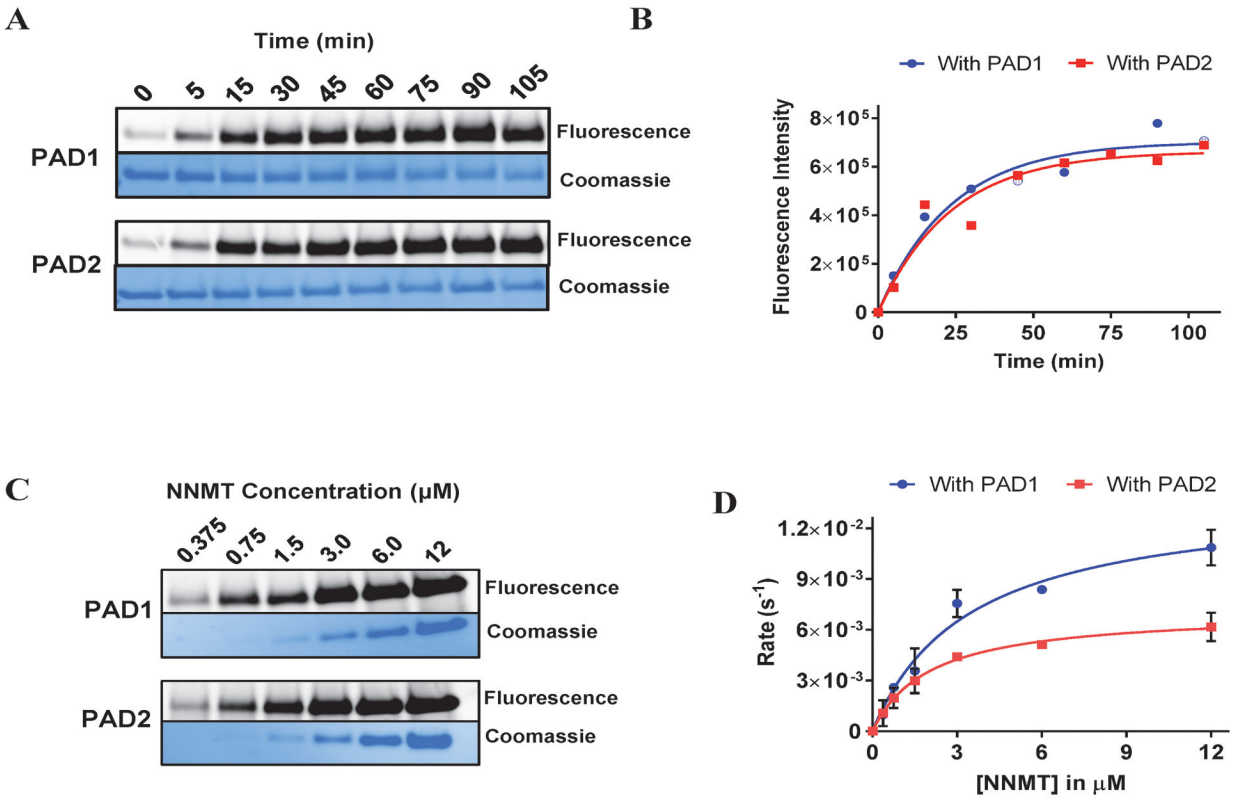

Figure 2.

(**A**) Time dependent citrullination of NNMT by PAD1 and PAD2 visualized by Rh-PG labeling. (**B**) Time courses of NNMT citrullination by PAD1 and PAD2 visualized by Rh-PG labeling. The data were fit to eq 2 (see methods). (**C**) Concentration dependent citrullination of NNMT by PAD1 and PAD2 visualized by Rh-PG labeling. (**D**) Michaelis-Menten plot showing the activity of PAD1 and PAD2 against NNMT.

A

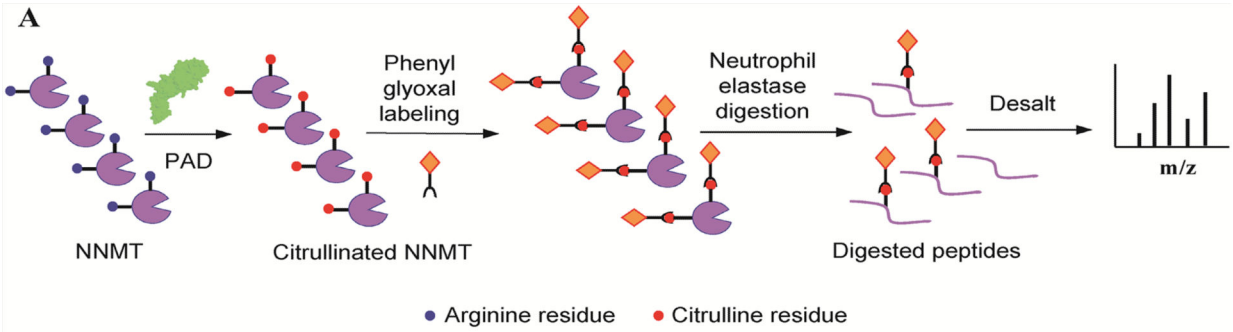

B

Residue	Peptide	Expected m/z[a]	Experimental m/z[a]
18	HFNP(Cit*)DYLEKYYKFGS	2181.008	2181.017
132	KGPEKEEKL(Cit*)QAV	1628.865	1628.865
181	L(Cit*)NLGSLLKPGGFLV	1587.890	1587.891

[a]Mass of citrulline include the +117.010 Da from the adduct with phenylglyoxal

C

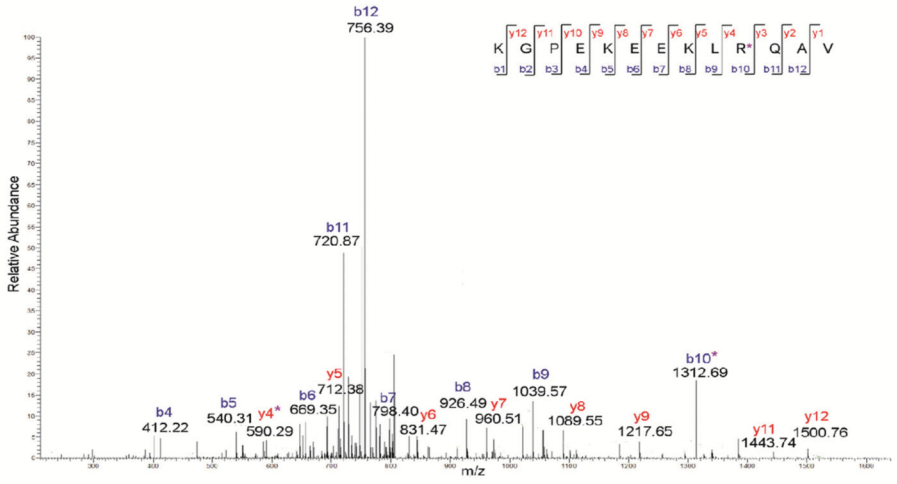

Figure 3.

(**A**) Workflow showing the labeling of citrullinated NNMT by phenylglyoxal and subsequent digestion with neutrophil elastase for the mass spectrometric detection of citrullinated peptides. (**B**) Table showing citrullinated peptides detected by mass spectrometry. Citrullinated residues are marked by an asterisk. The citrullinated residue number in NNMT is shown in the first column. (**C**) Representative MS/MS spectrum showing phenylglyoxal labeled NNMT at residue 132, which is citrullinated by PAD2.

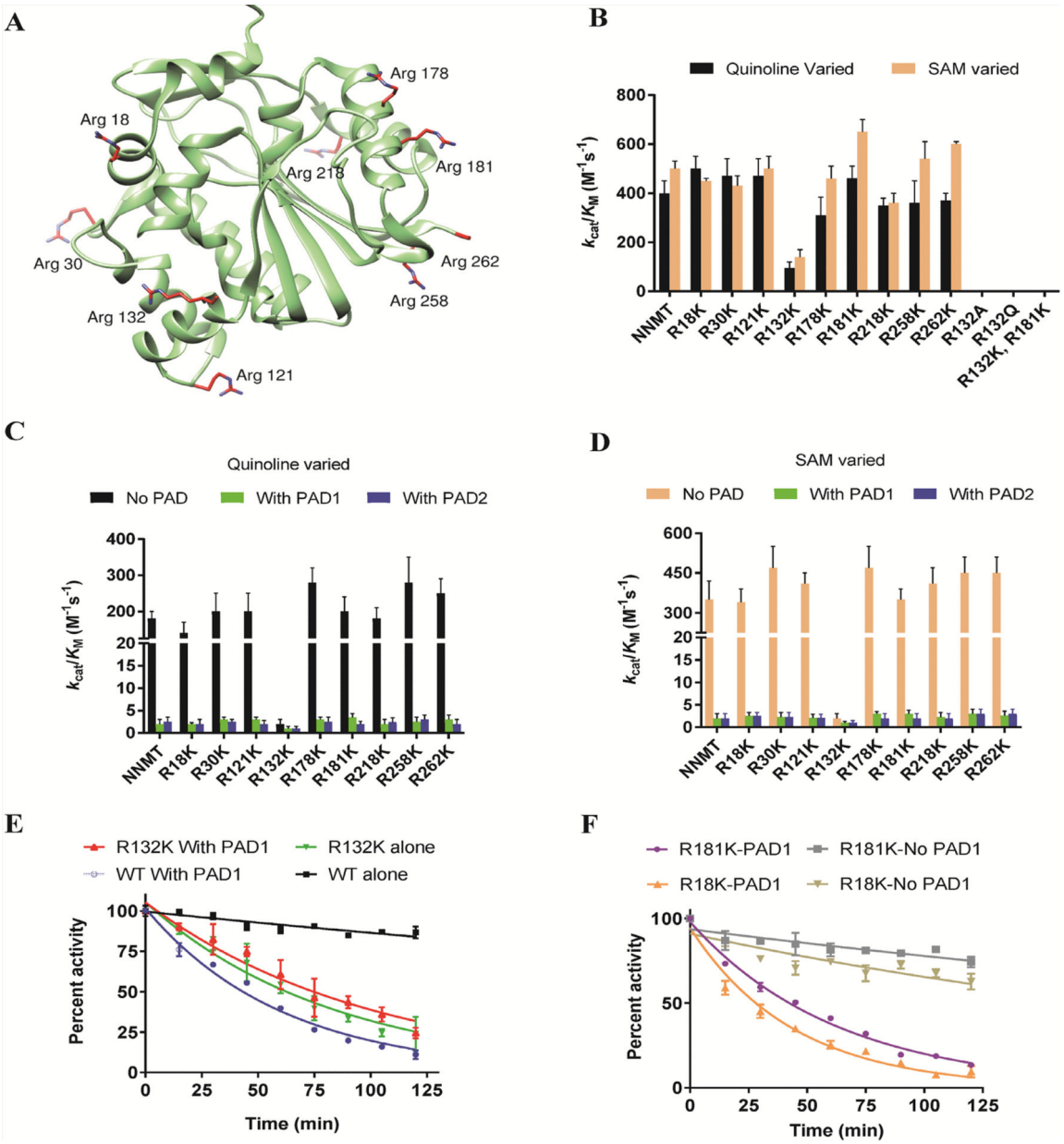

Figure 4.

(**A**) Ribbon representation (in green) of NNMT showing arginine residues in red (PDB code 3ROD). (**B**) Activity of NNMT and mutants measured using quinoline and SAM as substrates. (**C**) Time dependent citrullination of NNMT by PAD1 and PAD2 visualized by Rh-PG labeling. (**D**) Time courses of NNMT citrullination by PAD1 and PAD2 visualized by Rh-PG labeling. The data were fit to eq 2 (see methods). (**E**) Comparison of time dependent inactivation of WT and R132K as a result of PAD1 mediated citrullination. (**F**) Comparison of time dependent inactivation of R18K and R181K as a result of PAD1 mediated citrullination.

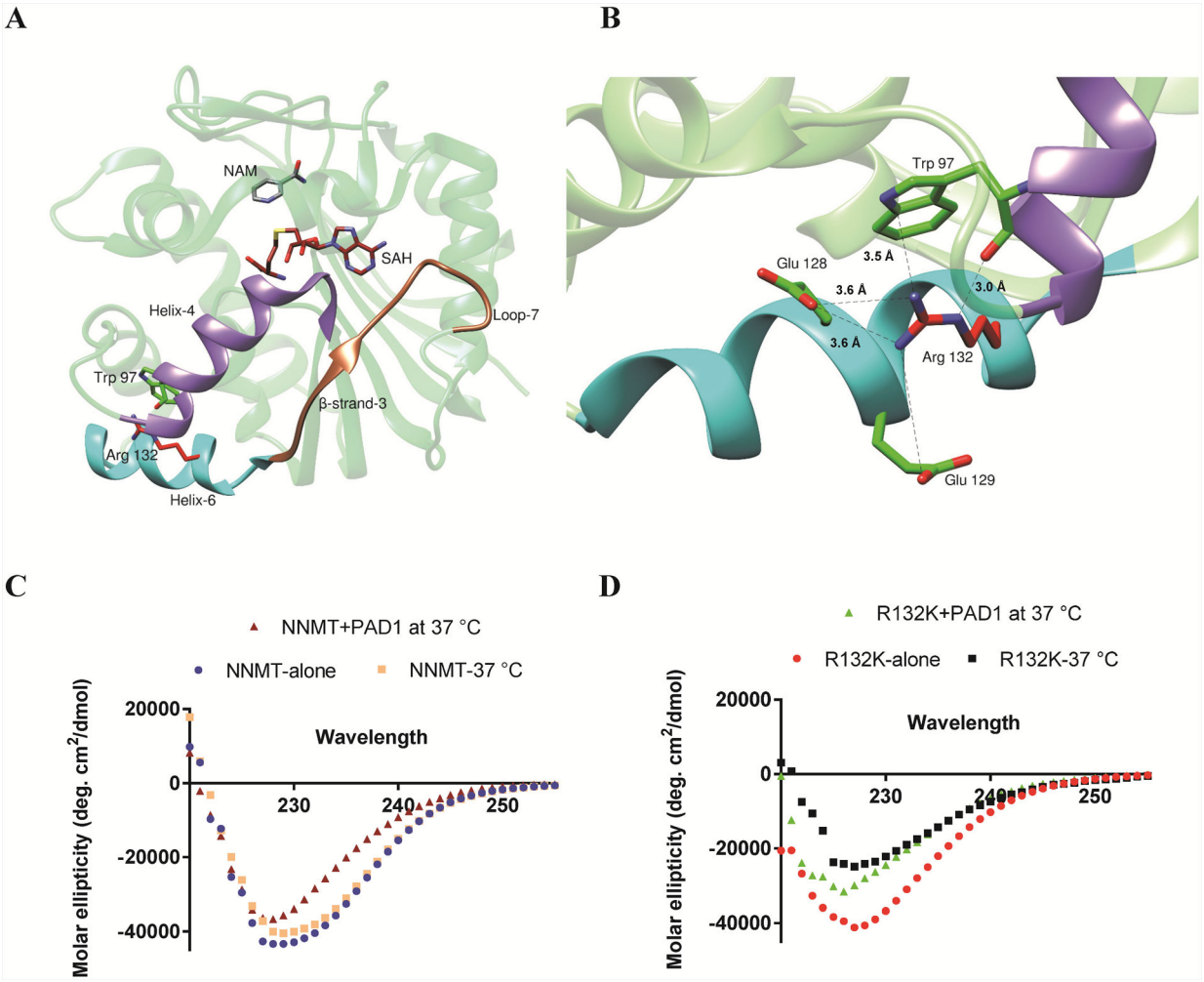

Figure 5.

(**A**) Ribbon structure of NNMT highlighting the active site loop (sienna) and helix 1 (purple). The residues in the loop and the helix interact with the cofactor SAM and are proposed to be essential for its binding at the active site. (**B**) Ribbon representation of NNMT depicting the interaction of R132 with W97 and E128. (**C**) CD spectra of citrullinated and uncitrullinated NNMT at 37 °C. The spectra of NNMT without incubation is shown for reference. (**D**) CD spectra of citrullinated and uncitrullinated NNMT-R132K at 37 °C. The spectra of NNMT without incubation is shown for reference.

Table 1.

Comparison of the rate of citrullination of NNMT mutants with their rate of inactivation.

	Rate of citrullination	Rate of NNMT inactivation with PAD1	Rate of NNMT inactivation No PAD1
Proteins	$k_{obs} \times 10^{-2}$ **(min^{-1})**	$k_{obs} \times 10^{-2}$ **(min^{-1})**	$k_{obs} \times 10^{-2}$ **(min^{-1})**
NNMT	4.0 ± 0.1	1.6 ± 0.1	0.10 ± 0.03
R18K	4.8 ± 0.6	2.3 ± 0.1	0.30 ± 0.06
R132K	5.0 ± 0.3	0.9 ± 0.1	1.2 ± 0.1
R181K	4.0 ± 0.2	1.6 ± 0.2	0.18 ± 0.03